Numerical Simulations of Oscillatory Cold Flows in an Axisymmetric Ramjet Combustor

Suresh Menon* and Wen-Huei Jou†
Quest Integrated, Inc., Kent, Washington 98032

A numerical simulation and analysis technique was developed to study the interaction between the vorticity component and the acoustic component of the flowfield in an axisymmetric ramjet combustor. To exclude the effects of the outflow boundary conditions, the interior of the combustor was isolated from the external region by a choked nozzle. The subsonic inflow boundary conditions are damping and thus do not force the oscillations. The shear layer separating at the step is perturbed by the low-frequency pressure fluctuation at the base of the step. The perturbation is then amplified downstream by the shear-layer instability and large-scale vortical structures are formed. When these structures impinge on the downstream nozzle wall, secondary vortices are generated, and large fluctuations in the Mach number upstream of the nozzle throat are observed. However, the Mach number in the supersonic region downstream of the throat remains stationary. The pressure and the vorticity spectra indicate the presence of the same low-frequency components, suggesting a possible vortex/acoustic wave interaction. Analysis of the computed mean-flow quantities and the higher moments indicates that, for the majority of the flow region, the large-scale structures are the main contributor to the transport of momentum. In a related study, the information obtained from these simulations is used to propose a model for one of the possible vortex/acoustic wave interactions.

Introduction

A SUBSTANTIAL research effort has been initiated to understand the mechanism for instability in ramjet combustor flowfields. This understanding can lead to the development of methods for suppressing the instability and, hence, to improvements in the performance of ramjet engines. Typically, the instability manifests itself in the form of large-amplitude pressure oscillations in the low-frequency range of a few hundred hertz. These pressure oscillations can cause structural damage or result in system failure caused by the expulsion of the inlet shock. The exact mechanisms of these self-excited oscillations are not entirely clear.

According to the linear canonical decomposition of the governing equations for small disturbances in an infinite compressible medium, three types of waves can be sustained in a moving medium: the vorticity wave, the entropy wave, and the two families of acoustic waves.[1] In a free space, these infinitesimal wave motions are linearly independent. In nonlinear cases and in a closed domain such as a ramjet combustor, however, these disturbances may interact through resonant phenomena and/or through boundary effects. Therefore, there is a fundamental question of how these wave phenomena may couple together in a finite bounded domain to form eigenmode oscillations with a discrete frequency spectrum. These eigenmodes are potential candidates for high-amplitude excitation when combustion occurs.

Eigenmode oscillations involving only one wave component have been explored extensively. The well-known acoustic duct modes are an example involving only acoustic waves. These oscillations, referred to as "resonant oscillations" in this paper and in a related study,[2] may be excited by distributed sources in a closed domain. The wall effects are included in the free-mode calculations for the resonant oscillations. An example including only vorticity waves can be found in the so-called edge-tone oscillations, which have been extensively studied experimentally[3-5] and have recently been numerically simulated by Ohring,[6] who considered the incompressible fluid. The interaction between an impinging vortex and the leading edge of a plate produces disturbances that provide the perturbation at the jet exit upstream for the initiation of a new vortex.[3] This upstream feedback mechanism in the incompressible flow occurs through the Biot-Savart induction. The feedback is instantaneous, as the speed of signal transmission in the incompressible limit is infinite.

The Biot-Savart induction is dynamically meaningful only in the incompressible limit, i.e., when the reduced frequency based on the speed of sound approaches zero, as given by

$$\frac{4fl}{c} \ll 1 \tag{1}$$

where l is the characteristic length of the domain of interest (considered as a quarter wavelength for acoustic waves), and c is the speed of sound. This criterion certainly cannot be met when the entire spectrum of turbulent flow fluctuation is considered. For example, the pressure fluctuations under a turbulent boundary layer were considered by Ffowcs Williams.[7] He showed that the low-frequency spectrum is dominated by the propagating acoustic waves. When the above condition is not satisfied, the transmission speed of flow information upstream is limited by the speed of sound, and there may be a phase difference between the signal at the source location and at the point of interest. Therefore, acoustic waves must be considered as part of the system. The resulting oscillation may consist of both convective components and acoustic components. This class of oscillation is referred to as "coupled-mode" oscillation in this paper and in a related study.[2] In a typical combustor, the reduced frequency is of the order of unity; therefore, the incompressible model is inappropriate.

Resonant acoustic modes excited by turbulent combustion have been studied as a mechanism for combustion instability.[8]

Presented as Paper 87-1421 at the AIAA 19th Fluid Dynamics, Plasma Dynamics, and Lasers Conference, June 8-10, 1987, Honolulu, HI; received Nov. 18, 1988; revision received Sept. 11, 1989.

*Senior Research Scientist. (Quest Integrated, Inc., was formerly Flow Research, Inc.)

†Vice President, Applied Mechanics Division; currently, Manager, CFD Development, Boeing Commercial Airplane Group, Seattle, WA.

In many cases, however, the frequency of the observed oscillations differs from the eigenfrequency of the acoustic duct modes. More complex physics involving convective waves, i.e., entropy waves and vorticity waves, may be the cause of the deviation. Entropy-wave/acoustic-wave coupling was suggested by Abouseif et al.[9] as a mechanism for combustion instability; however, the role of vortex shedding was not considered. In contrast to this model,[9] some experimental evidence points to the participation of vortex shedding in combustion processes.[10-12] The vorticity fluctuations may interact with the acoustic wave directly and may also affect combustion through their effects on mass and heat transport. The unsteady combustion related to vortex shedding may generate acoustic disturbances. Vortex shedding and vortex/nozzle interaction were suggested as part of the system important to combustion instability.[13] This possible coupling between acoustic waves and vortical disturbances prompted Crocco and Sirignano[14] to study theoretically the acoustic reflection coefficient of a choked nozzle subject to the impingement of a vortical disturbance. The study of vortex/acoustic interaction in a nozzle under a cold flow configuration, as in the theoretical work of Crocco and Sirignano,[14] is an essential first step toward untangling the intricate interactions among all the wave components leading to combustion instability.

The objective of this and the related study[2] is to understand the interaction between the vortex dynamics and acoustic waves in a generic combustor geometry. Since combustion is not considered in this investigation, a direct inference from the results of this investigation to the combustion instability is inappropriate. However, the basic understanding of the cold flow as well as the methodology developed in this investigation provides a sound basis for extending the analysis to a reacting flowfield. This is currently underway, and some results were recently reported.[15]

Because of the complexity of the problem, an analytical solution to the governing equations with complex boundary conditions is not possible. In particular, complex vortex merging processes and the resulting acoustic disturbances are difficult to analyze without using drastic approximations. Numerical simulations, if performed properly, may provide important information for understanding the physics. In this article, the development of a numerical methodology and methods for extracting physics from the simulations are reported. Detailed analysis of the simulation results to extract information on the vortex/acoustic interaction is discussed in a related study.[2]

Numerical Model

The governing equations are the unsteady, compressible Navier-Stokes equations:

$$\frac{\partial \rho}{\partial t} + \nabla \cdot \rho v = 0 \tag{2}$$

$$\frac{\partial (\rho v)}{\partial t} + \nabla \cdot (\rho v v + p\bar{I}) = \nabla \cdot \bar{\sigma} \tag{3}$$

$$\frac{\partial \rho E}{\partial t} + \nabla \cdot (\rho v H + q - v \cdot \bar{\sigma}) = 0 \tag{4}$$

where flow variables are given by their conventional notations and $\bar{I}$ is the identity diadics, $\bar{\sigma}$ is the shear stress tensor, q is the heat flux vector, E is the total energy, and H is the total enthalpy. These equations are supplemented by the following relations:

$$\bar{\sigma} = \mu(\nabla v + \tilde{\nabla} v) + \lambda \nabla \cdot v\bar{I} \tag{5}$$

$$q = -\kappa \nabla T \tag{6}$$

$$E = C_v T + 1/2\ v \cdot v \tag{7}$$

$$H = E + (p/\rho) \tag{8}$$

$$p = \rho R T \tag{9}$$

The above equations were solved using the axisymmetric approximation, which requires some justification. The objective of this study is to investigate the interaction between low-frequency pressure oscillations and the dynamics of large vortices in an axisymmetric ramjet combustor. The low frequency is usually associated with longitudinal acoustic waves, which are likely to propagate axisymmetrically. If large vortices are coupled to these acoustic waves, they are likely to be approximately axisymmetric. Although the small-scale turbulence is three-dimensional, it is assumed to provide only a dissipative mechanism to the large-scale phenomena. Whether the dynamics of the large-scale phenomena are critically dependent on the amount of dissipation can be examined later by varying the dissipation coefficients in the governing equations. At present, there is no validated subgrid model that can be used for compressible flows. The laminar dissipative coefficients used here can be viewed as a simple subgrid model, as noted by Ferziger and Leslie.[16] Therefore, the present simulation model does contain a degree of uncertainty. However, the model contains the essential physics of vortex/acoustic interaction.

The above equations were solved in a typical domain as shown in Fig. 1a. Boundary conditions and initial conditions are required to complete the description of the model. On all solid-wall boundaries, no-slip and adiabatic boundary conditions are applied, i.e.,

$$v = 0 \qquad \text{on solid surfaces} \tag{10}$$

$$n \cdot q = 0 \qquad \text{on solid surfaces} \tag{11}$$

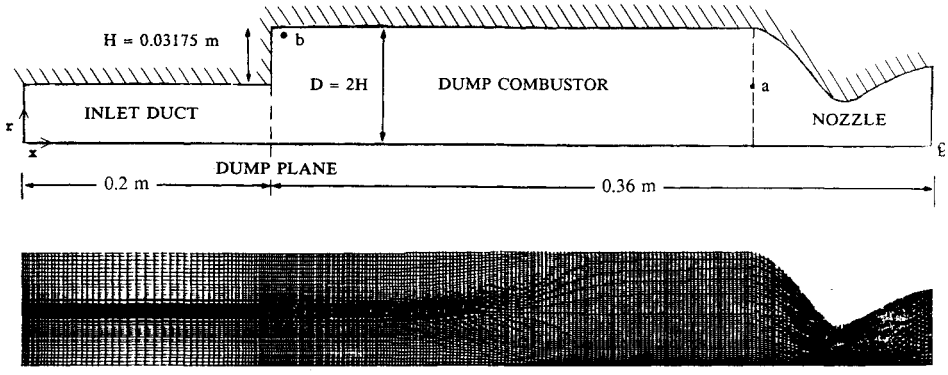

Fig. 1 Axisymmetric ramjet combustor: a) characteristic dimensions of the ramjet, b) 256×64 computational grid.

At the entrance of the inlet pipe, the flow is assumed to be in the axial direction with prescribed uniform stagnation pressure and stagnation temperature. The notion of "stagnation pressure" is not well defined in an unsteady flow. The application of these upstream conditions implies certain "impedance" conditions.[1] The characteristics of the impedance condition as applied here were examined by a linearized analysis,[2] and the condition was proven to be of the damping type. Therefore, the pressure disturbances that reach the inflow boundary will not be amplified and thus the computed sustained oscillation in the combustor is self-generated. Although the damping condition at the inflow boundary may affect the frequency and amplitude of the self-sustained oscillations, it may not affect the "basic" mechanism of the vortex/acoustic wave interaction in the combustor. It is conceivable that, in a practical ramjet device, the inlet diffuser oscillations such as those reported by Bogar and Sajben[17] may participate in the flow oscillations in the combustion chamber. Specific upstream impedance conditions can be derived if this kind of flowfield is completely understood. The effects of upstream impedance on the acoustic/vortex interaction problem have not been investigated in this study. The downstream boundary is at supersonic conditions, and thus no boundary conditions are required there. However, before the supersonic outflow is established, an exit pressure is initially specified. For the chosen inflow stagnation conditions and combustor dimensions, the specified exit pressure determines the Mach number at the inlet.

The initial condition is a quiescent flow with stagnation conditions everywhere in the flowfield. The exit pressure is then impulsively lowered to the prescribed value to start the flow. Once the flow is established, the exit pressure is further lowered to establish the supersonic flow downstream of the throat.[18] Subsequently, if required, the Mach number of the flow at the inlet can be changed by increasing or decreasing the nozzle throat area.

MacCormack's explicit, unsplit scheme[19] is used for the integration of the conservation equations in time. The scheme is second-order accurate in time and space. Its properties are well known and are described elsewhere.[18,19] The finite volume form of the scheme on a boundary-conforming grid was used. Aside from the well-known "built-in" artificial dissipation of the scheme, no explicit artificial dissipation has been added. Numerical stability of the time integration can be maintained with a Courant-Frederich-Levy number of 0.6.

A typical grid used in the simulations is shown in Fig. 1b. Grid lines are clustered in the critical regions such as the boundary layer in the inlet duct, the shear layer separation point (i.e., the corner of the backward-facing step), and the nozzle. These are the flow regions where the length scale of the flow features is expected to be small. The clustering of grid lines enables us to resolve the important large-scale features without an excessively large computational mesh. Large-scale structures with length scales of the order of the boundary-layer thickness or larger can be resolved. These are the large-scale vortical structures of interest in the present investigation.

Details of the simulation technique have been described previously.[18] Important features of the numerical model are summarized here. An important issue in numerical simulations of compressible flows is the effect of the boundary conditions on the solution inside the computational domain. If the outflow boundary is subsonic, boundary conditions are required there. If the local velocity vector is pointing outward, the vorticity and the entropy are convected outward. Among the two families of acoustic waves, one family propagates outward and carries the appropriate characteristic variable from the interior, but the other propagates inward representing the reflected wave on the outflow boundary. Therefore, one boundary condition must be supplied.

Again, this boundary condition represents an impedance condition, as was discussed previously for the inflow boundary. Unfortunately, unlike the fairly uniform inflow, the outflow is highly nonuniform and unsteady. The flowfield in the combustion chamber is then critically dependent on the arbitrary impedance condition for subsonic flows. Furthermore, a vortex in the subsonic outflow may exit at low speed causing locally reversed flow. In this case, the vorticity and the entropy are convected from downstream into the computational domain. Three boundary conditions are required there. These boundary conditions are difficult to specify and the resulting simulations are not reliable. In the present simulation model, the outflow boundary is at a supersonic state. Therefore, the flow inside the combustor is independent of the boundary conditions at the outflow boundary. A similar approach to isolating the combustor region from the outflow was used by other investigators,[20] who assumed a sonic outflow condition.

Two questions need to be addressed before the simulation model can be applied. The first is the question of grid resolution. Two sets of simulations were performed under identical flow conditions but using different grid resolutions. The first set of simulations used grids of 129×42 and 192×64, and the second set used grids of 129×42 and 256×64 with a slightly longer inlet duct.[18] The spectra of pressure fluctuation at the base of the step as well as the spectra of vorticity at the nozzle entrance are chosen as the basis for comparison. It was found that the coarser grid is able to produce nearly the same spectra as the finer grids with less than 10% difference in the spectral peaks.[18] However, the contour plots of the flow variables using the 129×42 grid lack the detail and smoothness of the higher-resolution simulations. All results presented here are based on simulations using either the 192×64 or the 256×64 grid.

The second question concerns the sensitivity of the observed spectra to the dissipation. Three simulations were performed with Reynolds numbers of 5,000, 10,000, and 33,000 (based on the inlet duct diameter and the freestream velocity). Increasing the Reynolds number causes a decrease in the thickness of the shear layer separating at the rearward-facing step and increases the vortex rollup frequency. However, the passage frequency of the merged large-scale structure downstream should not be dependent on the thickness of the shear layer. The comparison of the vorticity spectra at the nozzle entrance obtained from the different Reynolds number simulations[18] indicated that the dominant frequency varied less than 10%. This demonstrated that the passage frequency is not an intrinsic function of the shear layer. The comparison of the pressure spectra also showed that the results were insensitive to the variation of dissipation in that range.[18]

During simulations, flow quantities are monitored at various locations to determine whether the flow has reached a stationary oscillation. The data in the transient period are discarded before the analysis of the data in terms of the frequency spectra is performed. The numerical model constructed above is capable of capturing the essential large-scale unsteady phenomena of interest and can be used to study the vortex/acoustic interaction.

Large-Scale Unsteady Flow Structures

The vorticity dynamics of the flow inside the combustor can be visualized by a time sequence of vorticity contour plots as shown in Fig. 2. The boundary layer separates from the surface at the corner of the backward-facing step. The resulting free shear layer rolls up into concentrated vortices. Subsequently, these vortices merge several times to form large structures that impinge on the nozzle wall. As the vortices impinge on the wall, a secondary vortex of opposite sign is generated forming a vortex pair, which subsequently lifts itself away from the wall. These observations, which are consistent with the experimental observations of Didden and Ho,[21] indicate that strong acoustic radiation may result from the process of generating the secondary vortex.

The phase speed of the downstream-traveling vortical structures can be obtained by a two-point correlation analysis of

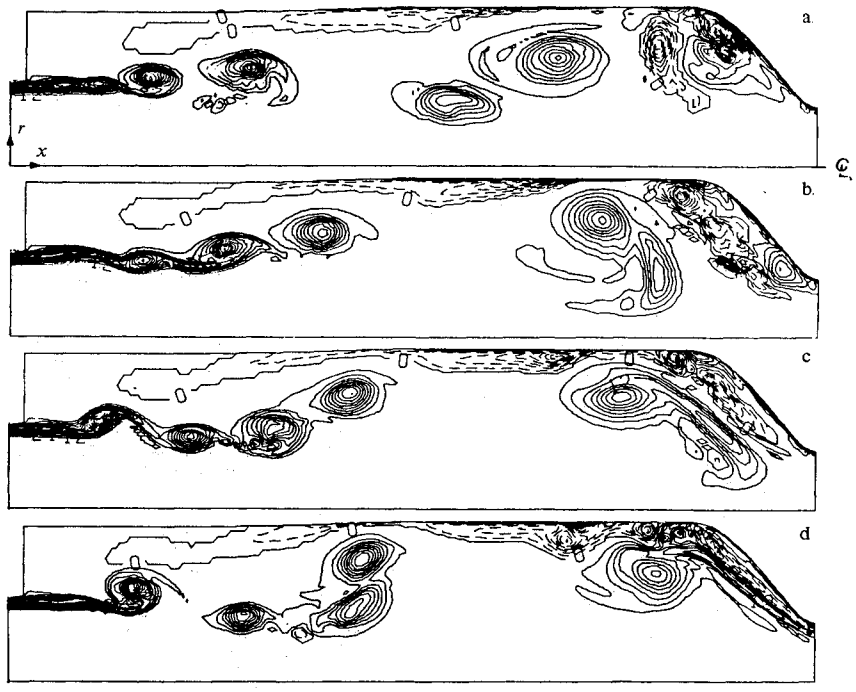

Fig. 2 Time sequence of vorticity contours in the combustor: the computational grid is 256 × 64, the contour interval is 3000 s^{-1}, the time interval between each figure is 0.32×10^{-3} s, the inlet Mach number is 0.32, and Re_D = 10,000.

the axial velocity fluctuation in the shear layer, i.e.,

$$R(\tau, \Delta x) = \frac{1}{T}\int \frac{u'(x,t)u'(x+\Delta x, t+\tau)\mathrm{d}t}{[R(x)R(x+\Delta x)]^{-1/2}} \qquad (12)$$

where $R(x)$ is the autocorrelation. The cross-correlation with the separation distance of $\Delta x \simeq 3.04$ cm was computed at the axial location $x/H = 4.65$, and another cross-correlation with a separation distance of $\Delta x = 7.86$ cm was computed at $x/H = 9.965$, as shown in Figs. 3a and 3b, respectively. The phase speed can be computed based on the most correlated τ and the separation distance Δx. The computed phase speeds for the upstream point (Fig. 3a) and the downstream point (Fig. 3b) are $0.61U$ and $0.52U$, respectively, where U is the speed in the inlet duct. The phase speed at the upstream location agrees with the experimental measurement of a free-jet. The lower phase speed downstream may be the result of the interference effect of the nozzle or the result of vortex merging.[22] The information on the phase speed of the vortical structures obtained here is used in a related study[2] for modeling the coupled-mode oscillation.

The frequency spectra of the vorticity fluctuations and the pressure oscillations at various locations in the combustor were analyzed. The frequency spectra shown in this article were obtained using a filter based on the maximum entropy method or MEM[18,23] to reduce the high-frequency noise that occurs during the Fourier transform of a finite time record. It is well known that, although the MEM analysis provides reliable information on the frequency content of the dominant oscillations, the relative amplitude of the frequencies may not be predicted accurately. Thus, the amplitude information in MEM-generated spectra is considered unreliable and is neither shown in the figures nor used in the analysis.

The vorticity spectra in the separated shear layer show high-frequency components related to the vortex merging process. Figure 4a shows the spectra in the shear layer around one step height downstream of the rearward-facing step. Three dominant peaks at 2.0 kHz, 1.74 kHz, and 647 Hz are present in these spectra. The frequency of the most unstable mode in the shear layer can be estimated at the step by using a Strouhal number ($St_\theta = f\theta/U$) of 0.017 and the computed momentum thickness θ. It was shown earlier[18] that the displacement thickness at the step oscillates in phase with the pressure perturbation. The momentum thickness at the step also oscillates. Using the computed momentum thickness variation at the step, the most unstable frequency ranges from 3.4 to 4.0 kHz. The high-frequency peaks at 1.74 and 2.0 kHz in Fig. 4a correspond closely to the first subharmonic of the most unstable shear-layer mode. The peak at 647 Hz is related to the acoustic fluctuations, as shown in a related study.[2]

Near the nozzle, the vortices merge into large structures at a frequency of 370 Hz, as shown in Fig. 4. If converted to a Strouhal number based on the jet diameter (i.e., $St = fD/U$), this frequency is approximately 0.2, which is within the range of reported "jet preferred mode" values of 0.2 to 0.7.[24] In a confined-jet configuration such as the ramjet combustor, the jet preferred mode may be more complex than for a freejet configuration due to the additional length scale, i.e., the length of the chamber involved. The selection of the preferred mode frequency from the possible range may depend on the axial length scale. Because there is no external perturbation imposed on the system and the computation is deterministic, this low-frequency, large vortical structure may be the result of a self-sustained mechanism. Several researchers[24-26] found that for a freejet, the acoustic disturbance generated during vortex merging may serve as a feedback mechanism for perturbing the shear layer at the jet exit. The analysis of the simulation results[2] suggests that the acoustic disturbance generated by vortex/choked-nozzle interaction is the feedback mechanism in the ramjet.

It is informative to examine the spectrum of the pressure fluctuation behind the backward-facing step. The vorticity fluctuation at the base of the step is low. Therefore, the pressure fluctuation there is considered to be an acoustic fluctuation, i.e., a fluctuation corresponding to the unsteady potential flow.[27,28] This spectrum shown in Fig. 5 contains three dominant peaks: a high peak at 647 Hz and two low-frequency components at 377 and 182 Hz. Subsequent analysis[2] showed that the peak at 647 Hz is the result of resonant acoustic oscillations, and the peaks at 377 and 182 Hz are due to the coupled-mode oscillations.

Two regions of the flowfield are of particular interest. The first region is the boundary layer near the step. This is a

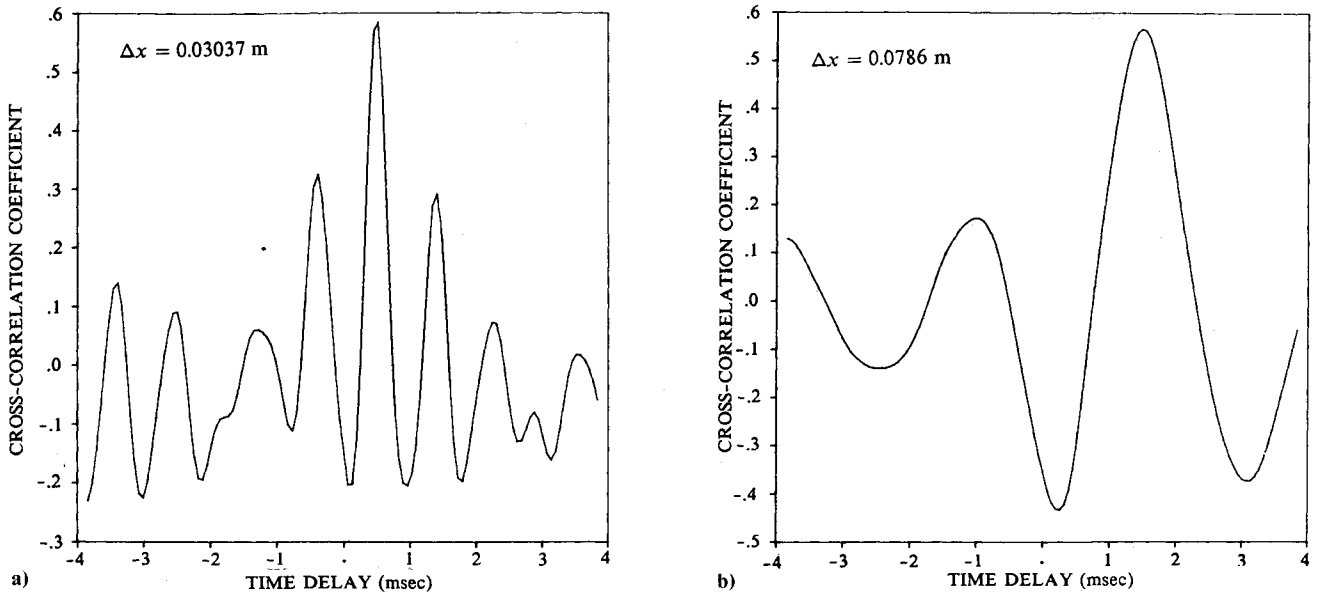

Fig. 3 Two-point cross-correlation of the axial velocity fluctuations, conditions same as in Fig. 2: a) cross-correlation near the dump plane, $x/H = 4.65$, b) cross-correlation near the nozzle, $x/H = 9.965$.

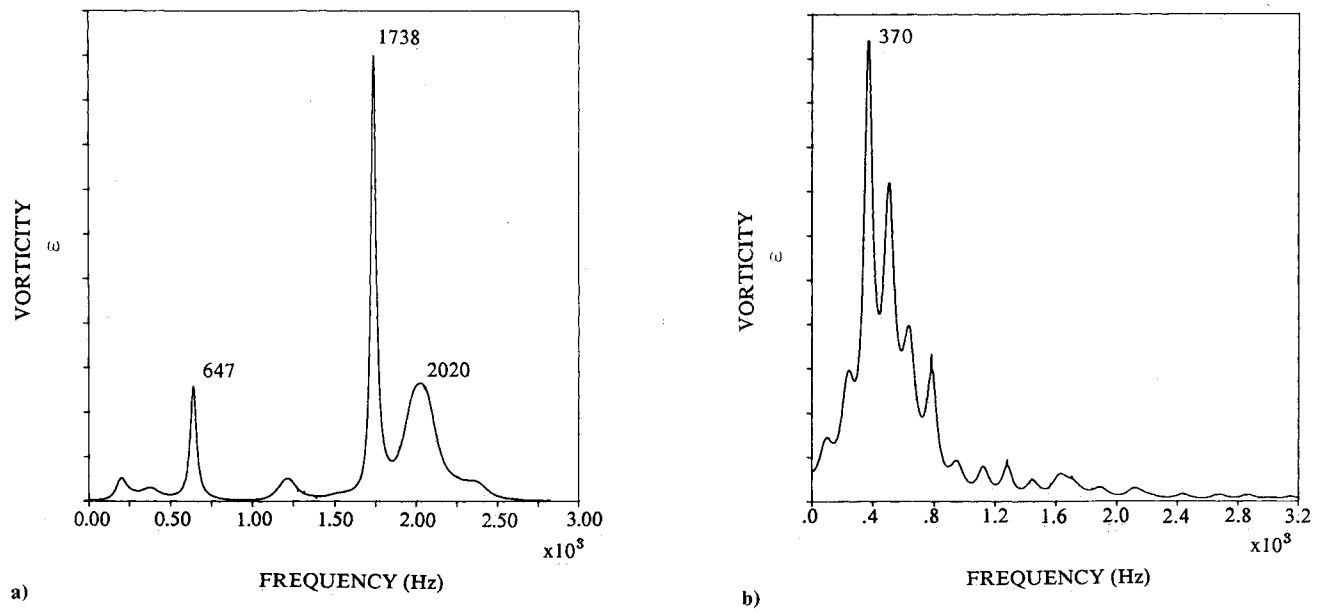

Fig. 4 Vorticity spectra in the combustor. The inlet Mach number is 0.32, $Re_D = 5000$, and the grid is 192×64: a) vorticity spectrum in the shear layer one-step height downstream of the step, b) vorticity spectrum at the nozzle entrance.

sensitive region in which the downstream disturbance may propagate upstream to interact with the corner and perturb the separating shear layer. The other is the nozzle region where the flow is choked. An unsteady disturbance interacting with a choked nozzle will generate upstream-propagating flow perturbations.

At a cross section slightly upstream from the corner of the step, the time history of the displacement thickness was computed. The displacement thickness of the boundary layer at the step corner and the pressure oscillation at the base of the step were compared.[18] The boundary-layer thickness was shown to fluctuate in phase with the pressure fluctuation. The displacement thickness at various upstream stations in the inlet was also computed. The amplitude of the fluctuation in the displacement thickness quickly diminishes upstream of the corner. The length scale of the decay is of the order of a few boundary-layer thicknesses. This seems to indicate that the fluctuation in the inlet duct boundary layer is the result of the interaction between the pressure fluctuation behind the step and the corner where the flow is separating. It is not the result of any fluctuation occurring in the flow upstream of the step.

The interaction of the impinging vortex and the choked throat can be visualized by the time sequence of vorticity contour plots and the corresponding Mach number contour plots shown in Figs. 6a and 6b, respectively. As the large structures impinge on the nozzle wall, secondary vorticity of the opposite sign is generated. This was also observed by Didden and Ho.[21] As can be seen, the Mach number contours in the subsonic portion of the nozzle fluctuate significantly during the period of vortex/nozzle interaction. In the cold flow computed here, the fluctuation in the static temperature is not very large. Thus, the fluctuation in the Mach number is

due to significant fluctuations in the velocity. The Mach number contours, however, remain relatively stationary in the supersonic region. The location and the shape of the sonic line also remains relatively unaffected during the vortex/nozzle interaction. The observed unsteady disturbance in the subsonic portion of the nozzle interacts with the choked throat and generates upstream propagating perturbations. This observation is in agreement with the analysis by Flandro.[29] Although the flowfield near the throat is highly two-dimensional and nonlinear, the computed results seem to support the assumption of a steady sonic throat made by Marble and Candel[30] and by Crocco and Sirignano[14] for the simplified analysis of the nozzle impedance. The acoustic impedance of a choked nozzle subject to an impinging vortex is discussed further by Jou and Menon.[2]

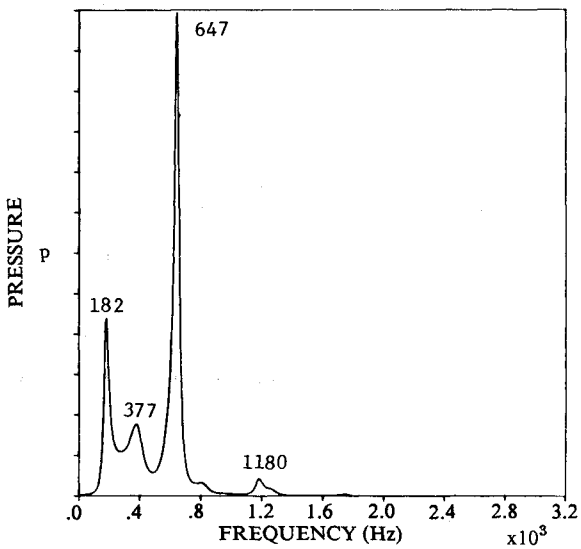

Fig. 5 Pressure spectrum at the base of the step, conditions same as in Fig. 4.

Mean Flow

In a large-eddy simulation, the dynamics of the coherent structures in a turbulent flow is captured by the unsteady computation. If sufficiently long time-accurate data are available, the time-averaging process provides a means to evaluate the contributions of these large structures to the transport of mass and momentum. Therefore, the mean-flow variables and the higher moments are computed by time averaging the instantaneous variables. If experimental data are available, the mean flow quantities and higher moments computed can be compared to the data to assess whether the main characteristics of the flow are faithfully simulated. Because of the lack of comprehensive experimental data for a circular jet in a sudden expansion (i.e., a backward-facing step), the available mean-flow data for flows past a primarily two-dimensional backward-facing step[31-40] were used to make some qualitative comparisons with the present computational results. There are obvious differences between the present computations and the experiments, such as the geometry, the downstream nozzle, and the flow conditions; however, the time-averaged flowfields without combustion instability may be qualitatively similar away from the nozzle region. Furthermore, although acoustic waves are present in the present study, the acoustics are weak and can only couple with the shear-layer separating at the sharp corner.

Figure 7a shows the nondimensional mean axial velocity profiles $\bar{u}/U$ as a function of the axial locations x/H in a combustor. Only the region between the dump plane ($x/H=0$) and the nozzle entrance ($x/H \approx 8$) is shown in this figure. The experimentally obtained profiles[31] are also shown in this figure. The agreement between the computational re-

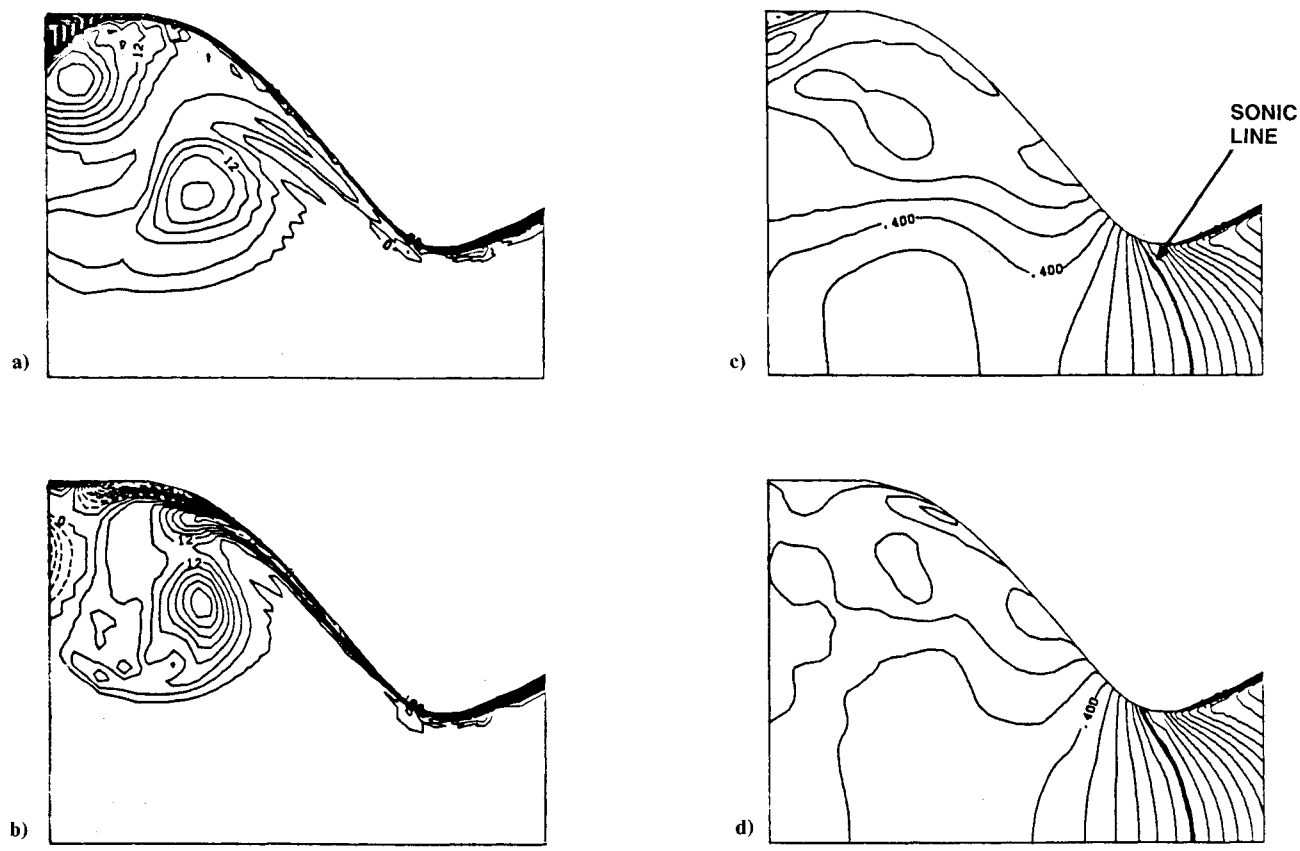

Fig. 6 Time sequence of vorticity contours (at interval of 3000 s^{-1}) and Mach number contours (at interval of 0.1) in the nozzle, conditions same as in Fig. 2: a-b) Vorticity contours, c-d) Mach number contours.

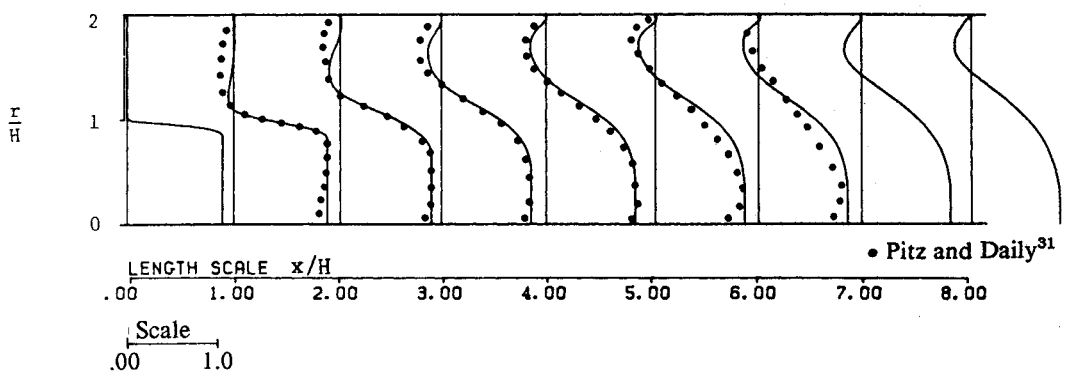

a)

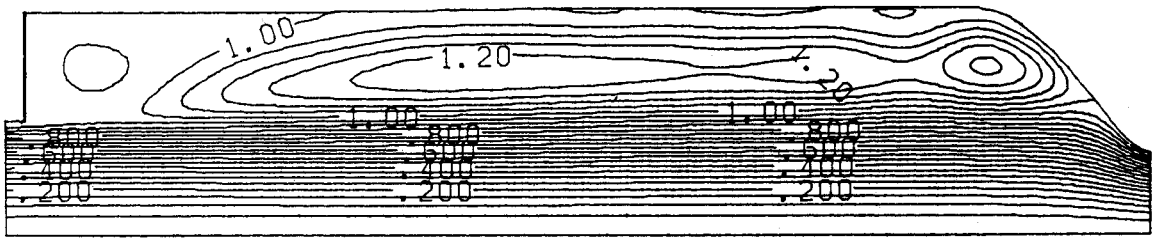

b)

Fig. 7 Axial mean velocity profiles and mean streamlines in the combustor; conditions same as in Fig. 2: a) streamwise mean velocity profiles, $\bar{u}/U$, b) normalized stream function, ψ.

sults and the experiments for $x/H < 4$ is good. For $x/H > 5$, the spreading rate of the shear layer in experiments is much faster than the computed results. Several factors may contribute to this difference between the experimental results and the computational results. First, the three-dimensional breakdown of the vortical structure, which cannot be modeled by an axisymmetric computation, may become important at the downstream location. Also, the difference between an axisymmetric and a planar configuration may become prominent at the downstream location where the coherent ring vortices are stretched due to the radial motion. The maximum reversed axial velocity in the recirculation region is approximately $0.21U$, which is within the experimentally observed range of $0.2U$–$0.25U$.[32-34]

The mean stream function ψ can be obtained by solving the following equations:

$$\overline{\rho u}\, r = \frac{\partial \psi}{\partial r}, \qquad \overline{\rho v}\, r = -\frac{\partial \psi}{\partial x} \tag{13}$$

subject to the appropriate boundary conditions, i.e.,

$$\psi = 0 \text{ at the center line } (r = 0) \tag{14}$$

$$\psi = 1 \text{ on the solid wall} \tag{15}$$

where ψ is normalized by the mass flux across the upstream inflow boundary. Figure 7b shows the mean streamline pattern. Within the elongated recirculation zone, a closed streamline domain with a freestanding stagnation point near the nozzle is indicated. A secondary recirculation zone near the step, with a circulation opposite to the primary recirculation zone, is also observed. The secondary recirculation zone has been reported in many previous experiments.[32,35,36]

The shear-layer spreading rate can be estimated by using the vorticity thickness defined by

$$\delta_w = \frac{\Delta U}{\left|\frac{\partial \bar{u}}{\partial r}\right|_{\max}} \tag{16}$$

where $\Delta U = (U_1 - U_2)$, which is the difference in mean axial velocity across the shear layer. We chose $U_2 = 0$, which approximates the mean velocity at the base of the step. Figure 8 shows the computed results along with some experimental results.[31] The shear-layer spreading rate $d\delta_w/dx$ in the region $x/H < 3$ is approximately 0.24. The experimental values of 0.26 to 0.29 were reported by Pitz and Daily,[31] whereas a lower rate is reported by Eaton and Johnston.[33] The values reported for the backward-facing step configuration are substantially higher than the spreading rate of 0.125 to 0.20 reported by Gutmark and Ho[24] for a freejet. Beyond $x/H > 5$, the size of the coherent structures is comparable to the step height, and the spreading of the shear layer is inhibited by the wall.

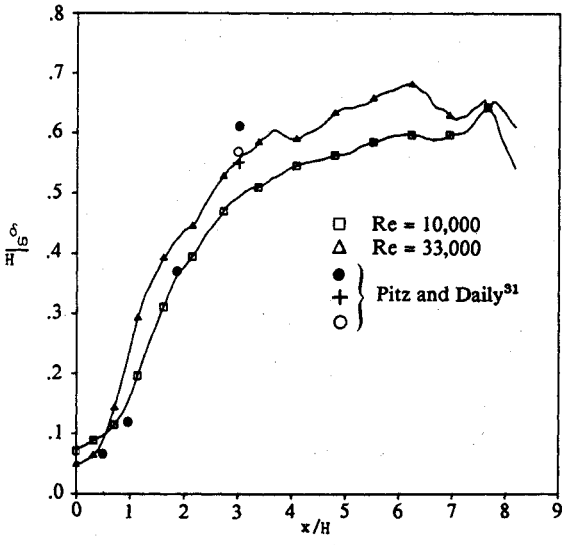

Fig. 8 Axial variation of vorticity thickness in the combustor.

The Reynolds stress tensors $\overline{u_i' u_j'}$ were also evaluated. Figures 9a and 9b present the profiles of the streamwise fluctuation intensity $\sqrt{(u'^2)}/U$ and the traverse fluctuation intensity $\sqrt{(v'^2)}/U$, respectively, for the Re = 10,000 simulation. Some experimental data[31] are also shown. A few observations are important. The fluctuation of the longitudinal velocity is quite

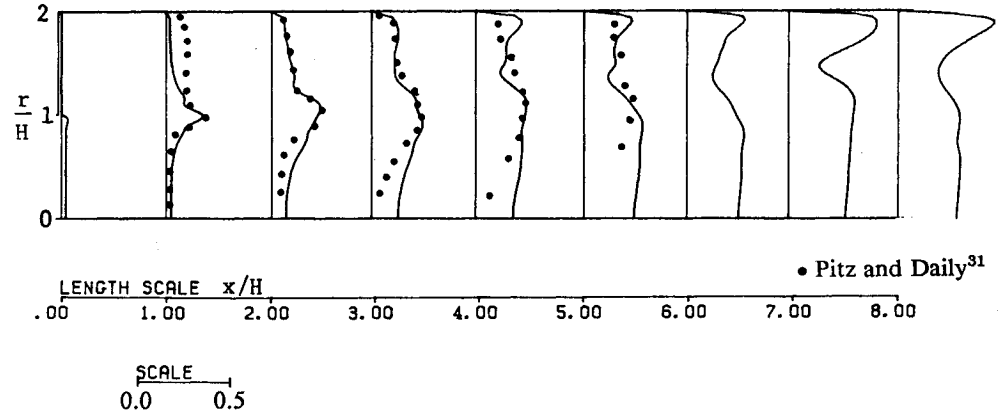

a)

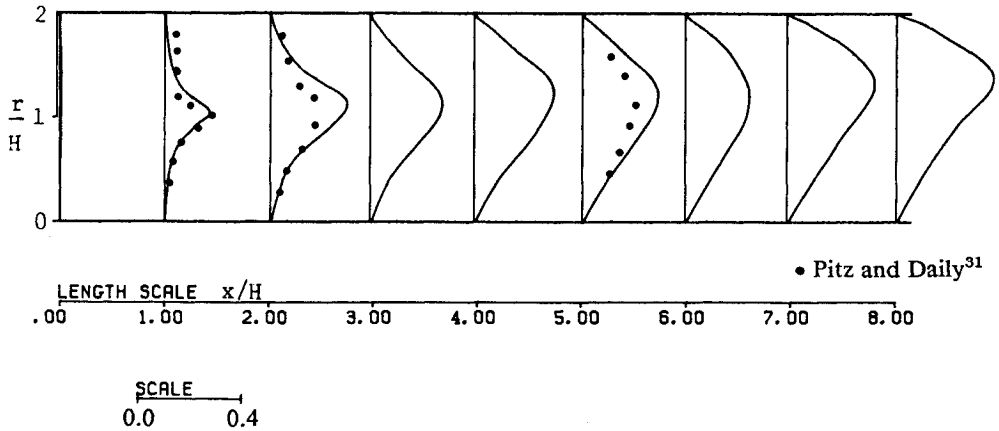

b)

Fig. 9 Axial variation of the velocity fluctuation intensity in the combustor; conditions same as in Fig. 2: a) streamwise fluctuation intensity ($\sqrt{u'^2}/U$) profiles in the combustor, b) transverse fluctuation intensity ($\sqrt{v'^2}/U$) profiles in the combustor.

intense along the axis of the combustor, whereas the mean velocity profiles in Fig. 7a show no decay of the mean axial velocity. Along the axis, the fluctuation in axial velocity is the result of the induced flow by the passage of the coherent vortex ring. It does not contribute to the momentum transport across the cross sections. Hence, there is a strong velocity fluctuation even in the potential core in an axisymmetric case. Using the results of the three Reynolds number simulations, the peak value of the streamwise fluctuation $(\overline{u'^2})_{max}/U^2$ in the shear layer is estimated in the range of 0.04 to 0.06,[18] which appears to agree with the reported value of around 0.04.[35] The global maximum occurs near the dump wall at $x/H \approx 8$, about one step height upstream of the impingement point, and then decreases in the downstream direction through the nozzle throat.[18] These numerically computed results are consistent with past experimental observations.[33,37]

Figure 10 shows the variation of the peak shear stress, $-(\overline{u'v'})_{max}/U^2$, as a function of axial location. The maximum value of the shear stress increases to a global peak at the location $x = 2.5H$ for the $Re = 5000$ simulation. With an increase in Reynolds number, this peak value increases, and the location shifts closer to the dump plane. This peak shear stress occurs in the region where, in an average sense, the primary vortices undergo pairing. Since the increase in Reynolds number results in a thinner and more unstable initial shear layer, the roll-up and pairing also occur closer to the dump planes, resulting in the shift of the peak shear stress closer to the dump plane. For comparison, some experimental data[38-40] are shown in this figure. Beyond $x = 2H$, the peak value of the shear stress begins to decrease, reaching a local minimum at $x \approx 5H$, after which it starts to increase again to reach another maxi-

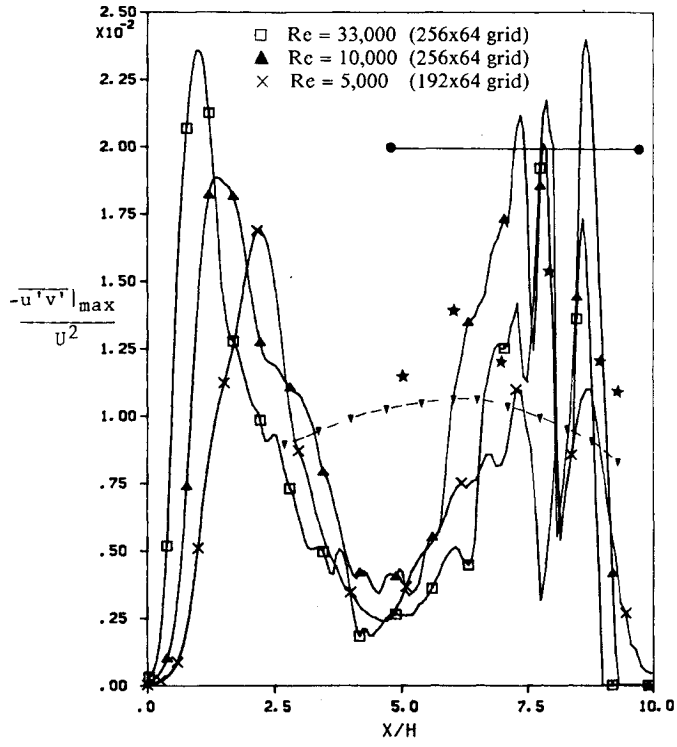

Fig. 10 Axial variation of peak Reynolds stress $-\overline{u'v'}|_{max}/U^2$ in the combustor; * Durst and Tropea,[38] ●—● Arie and Rouse,[40] ▼ – ▼ best estimate curve.[39]

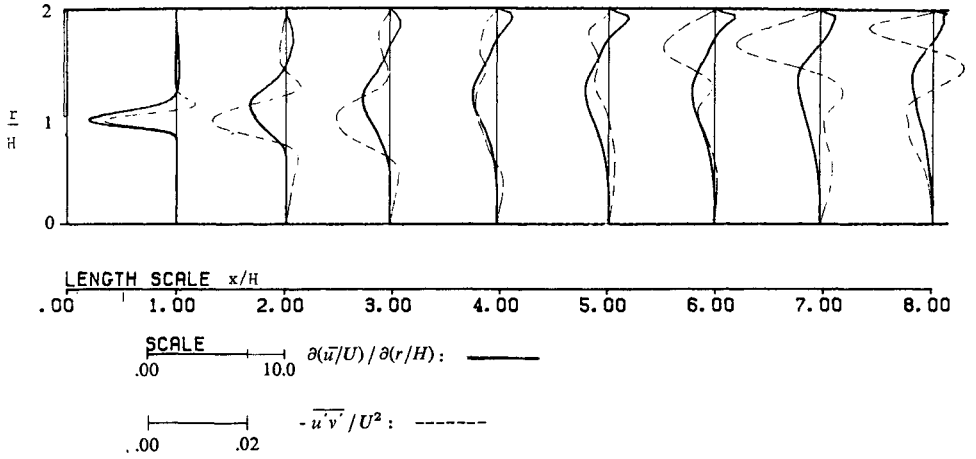

Fig. 11 Comparison of the profiles of the slope of streamwise mean velocity $\partial\bar{u}/\partial r$ and the Reynolds stress $-\overline{u'v'}/U^2$; conditions same as in Fig. 2.

mum in the impingement region. A maximum of 0.022 at $x \approx 2H$ is observed. The observed increase in Reynolds stress during pairing and its subsequent decrease thereafter is consistent with experimental observation.[25,41]

The Reynolds shear stress profiles change their sign in the transverse direction. Figure 11 shows the transverse profiles for the nondimensional mean velocity gradient $\partial\bar{u}/\partial r$ superimposed on the profiles for the shear stress, $-\overline{u'v'}/U^2$. Comparison of these two sets of profiles indicates that the shear stress and the slope of the mean profile have opposite signs in the recirculation zone, thus indicating a region of countergradient diffusion of momentum. Countergradient diffusion is also observed in the region around $x \approx 7H$ across nearly the entire cross section. Thus, the gradient hypothesis of the Reynolds stress closure—i.e., $-\overline{u'v'} = \nu_t \partial\bar{u}/\partial r$, where ν_t is the eddy viscosity—is clearly not generally applicable in the combustor. Countergradient diffusion, which implies a transfer of energy from the fluctuations back to the mean flow, has been experimentally observed and is a direct consequence of the presence of large-scale coherent structures (e.g., Hussain[41]). Countergradient diffusion has been shown to occur during pairing processes. This experimentally observed relationship between large-scale structure and shear stress variation is also seen in the present numerical simulations. In Fig. 10, for example, there is a peak in Reynolds stress at $x/H \approx 2$, which is near the region where the first pairing occurs. In this region, cogradient production of kinetic energy dominates with only small local regions of countergradient production. Further downstream, the maximum in the shear-stress distribution decreases in the shear layer as the pairing is completed and more regions of countergradient diffusion appear. The peak shear stress increases again as the second merging process occurs, which results in the large structure observed in the region $x/H \approx 7$. Near the dump wall, there is a small region where countergradient diffusion always appears to dominate.

Concluding Remarks

This article presents a numerical model for simulations of self-sustaining oscillatory cold flows in a ramjet configuration. In the simulations, no external forcing was imposed. Low-frequency and low-amplitude pressure oscillations as well as complex vortex merging processes were observed. The observed oscillatory flow is self-sustaining in nature. To study the dynamics of the flowfield, a detailed data reduction package has been developed that includes flow visualization, time averaging, and spectral analysis. A major issue in the development of an unsteady simulation model for compressible flows has been resolved in the present investigation. It was found that if the flow at the exit plane of the computational domain is subsonic, the interior solution depends on the boundary conditions imposed at the exit plane. When the exit nozzle is choked, no signal can propagate upstream from the supersonic exit plane. Therefore, the flowfield inside the combustor is independent of the exit condition and is faithfully simulated. This conclusion is important for any compressible flow simulation where a family of acoustic waves may propagate upstream against the subsonic flow. The grid resolutions of the simulations have been verified through a self-consistency check on the frequency spectrum. The unsteady flow features computed in the simulations can now be analyzed to uncover the underlying physical processes with some reasonable confidence.

The dynamics of the large-scale motion computed in the simulations is in reasonable agreement with experimental observation. The time-averaged data indicate that the coherent structures play a dominant role in the transport of momentum. The simulations and the results discussed in this article are used to develop techniques to extract acoustic information from the data and to identify the mechanism that leads to the observed oscillations.[2]

Acknowledgments

The present work is supported by the Office of Naval Research under Contract No. N00014-84-C0359. This research would not have been possible without the generous computational support from NASA Lewis Research Center on the CRAY-XMP computer, and from the National Aerodynamics Simulator (NAS) at NASA Ames Research Center for the higher-resolution computations. The authors would like to thank Robert MacCormack of Stanford University for providing the preliminary computer code. Discussions with M. Gaster of Cambridge University, England, clarified the need for using the MEM spectral analysis to reduce the noise in the spectra. The MEM analysis package was provided to us by C.-M. Ho of the University of Southern California, which we gratefully acknowledge.

References

[1]Chu, B.-T., and Kovasznay, L.S.G., "Nonlinear Interactions in a Viscous Heat-Conducting Compressible Gas," *Journal of Fluid Mechanics*, Vol. 3, 1958, pp. 494-514.

[2]Jou, W.-H., and Menon, S., "Modes of Oscillation in a Non-Reacting Ramjet Combustor Flow," *Journal of Propulsion and Power*, Vol. 6, No. 5, 1990.

[3]Rockwell, D., and Naudascher, E., "Self-Sustained Oscillations of Impinging Free Shear Layers," *Annual Review of Fluid Mechanics*, Vol. 11, 1979, pp. 67-94.

[4]Knisely, C., and Rockwell, D., "Self-Sustained Low-Frequency Components in an Impinging Shear Layer," *Journal of Fluid Me-*

chanics, Vol. 116, 1982, pp. 157–186.

[5]Staubli, T., and Rockwell, D., "Interaction of an Unstable Planar Jet with an Oscillating Leading Edge," *Journal of Fluid Mechanics,* Vol. 176, 1987, pp. 135–167.

[6]Ohring, S., "Calculations of Self-Excited Impinging Jet Flows," *Journal of Fluid Mechanics,* Vol. 163, 1986, pp. 69–98.

[7]Ffowcs Williams, J. E., "Boundary Layer Pressures and the Corcos Model: A Development to Incorporate Low Wave-Number Constraints," *Annual Review of Fluid Mechanics,* Vol. 125, 1982, pp. 9–25.

[8]Williams, F. A., *Combustion Theory, 2nd ed*, Benjamin/Cummings Publishing Co., CA, 1985.

[9]Abouseif, G. E., Keklak, J. A., and Toong, T. Y., "Ramjet Rumble: The Low-Frequency Instability Mechanism in Coaxial Dump Combustors," *Combustion Science and Technology,* Vol. 36, 1984, pp. 83–108.

[10]Schadow, K. C., Gutmark, E., Parr, T. P., Parr, D. M., and Wilson, K. J., "Large-Scale Structure as a Driver of Combustion Instability," AIAA Paper 87-1326, 1987.

[11]Keller, J. O., Vanevald, L., Korschelt, D., Hubbard, G. L., Ghoniem, A. F., Daily, J. W., and Oppenheim, A. K., "Mechanism of Instabilities in Turbulent Combustion Leading to Flashback,"*AIAA Journal,* Vol. 20, 1982, pp. 254–262.

[12]Smith, D. A., and Zukoski, E. E., "Combustion Instability Sustained by Unsteady Vortex Combustion," AIAA Paper 85-1248, 1985.

[13]Crocco, L., and Cheng, S.-I., "Theory of Combustion Instability in Liquid Propellant Rocket Motors," Buttersworths Scientific Publication, AGARDograph No. 8, 1956.

[14]Crocco, L., and Sirignano, W. A., "Behavior of Supercritical Nozzles Under Three-Dimensional Oscillatory Conditions," NATO, AGARDograph No. 117, 1967.

[15]Menon, S., and Jou, W.-H., "Large-Eddy Simulations of Combustion Instability in an Axisymmetric Ramjet Combustor," AIAA, Paper 90-0267, Jan. 1990; (accepted for publication in *Combustion Science and Technology*).

[16]Ferziger, J., and Leslie, D. C., "Large-Eddy Simulation: A Predictive Approach to Turbulent Flow Computation," AIAA Paper 79-1471, 1979.

[17]Bogar, T. J., and Sajben, M., "The Role of Convective Perturbations in Supercritical Inlet Oscillations," Chemical Propulsion Information Agency, Applied Physics Lab., Laurel, MD. *CPIA Publication No. 412,* Vol. 1, 1979, p. 465.

[18]Menon, S., and Jou, W.-H., "Simulations of Ramjet Combustor Flow Fields: Part 1—Numerical Model, Large-Scale and Mean Motions," AIAA Paper 87-1421, 1987.

[19]MacCormack, R. W., "The Effect of Viscosity in Hyper-Velocity Impact Cratering," AIAA Paper 69-354, 1969.

[20]Kailasanath, K., Gardner, J. H., Boris, J. P., and Oran, E., "Acoustic-Vortex Interactions and Low-Frequency Oscillations in Axisymmetric Combustors," AIAA Paper 87-0165, 1987.

[21]Didden, N., and Ho, C.-M., "Unsteady Separation in a Boundary Layer Produced by an Impinging Jet," *Journal of Fluid Mechanics,* Vol. 160, 1985, pp. 235–256.

[22]Stanaway, S. K., Cantwell, B. J., and Spalart, P. R., "Navier-Stokes Simulations of Axisymmetric Vortex Rings," AIAA Paper 88-0318, 1988.

[23]Andersen, N., "On the Calculation of Filter Coefficients for Maximum Entropy Spectral Analysis," *Geophysics,* Vol. 39, 1974, pp. 69–72.

[24]Gutmark, E., and Ho, C.-M, "Preferred Modes and the Spreading Rates of Jets," *Physics of Fluids,* Vol. 26, 1983, pp. 2932–2938.

[25]Ho, C.-M., and Huerre, P., "Perturbed Free Shear Layers," *Journal of Fluid Mechanics,* Vol. 16, 1984, pp. 365–424.

[26]Laufer, J., and Monkewitz, P. A., "On Turbulent Jet Flows: A New Perspective," AIAA Paper 80-0962, 1980.

[27]Crow, S. C., "Aerodynamic Sound Emission as a Singular Perturbation Problem," *Studies in Applied Mathematics,* Vol. 49, 1970, pp. 21–44.

[28]Goldstein, M. E., *Aeroacoustics,* McGraw-Hill, New York, 1976.

[29]Flandro, G. A., "Vortex Driving Mechanism in Oscillatory Rocket Flows," *Journal of Propulsion and Power,* Vol. 2, No. 3, 1986, pp. 206–214.

[30]Marble, F. E., and Candel, S. M., "Acoustic Disturbance from Gas Non-Uniformities Convected Through a Nozzle," *Journal of Sound and Vibration,* Vol. 55, 1977, pp. 225–243.

[31]Pitz, R. W., and Daily, J. W., "Combustion in a Turbulent Mixing Layer Formed at a Rearward-Facing Step," *AIAA Journal,* Vol. 21, 1983, pp. 1565–1570.

[32]Moss, W. D., Baker, S., and Bradbury, L. J. S., "Measurements of Mean Velocity and Reynolds Stresses in Some Regions of Recirculating Flow," *Turbulent Shear Flows I,* edited by L. B. J. Bradbury et al., Springer-Verlag, New York, 1979.

[33]Eaton, J. K., and Johnson, J. P., "A Review of Research on Subsonic Turbulent Flow Reattachment," *AIAA Journal,* Vol. 19, 1981, pp. 1093–1100.

[34]Kim, J., Kline, S. J., and Johnston, J. P., "Investigation of a Reattaching Turbulent Shear Layer: Flows over a Backward-Facing Step," *ASME Journal of Fluids Engineering,* Vol. 102, 1980, pp. 302–308.

[35]Durst, F., and Schmitt, F., "Experimental Studies of High Reynolds Number Backward-Facing Step Flow," *Turbulent Shear Flows 5*, edited by I. Durst et al., Springer-Verlag, Berlin, 1987.

[36]Minh, H. H., and Chassaing, P., "Pertubations of Turbulent Pipe Flow," *Turbulent Shear Flows I*, edited by L.B.J. Bradbury et al., Springer-Verlag, New York, 1979.

[37]Bradshaw, P., and Wong, F. Y. F., "The Reattachment and Relaxation of a Turbulent Shear Layer," *Journal of Fluid Mechanics*, Vol. 52, 1972, pp. 113–135.

[38]Durst, F., and Tropea, C., "Turbulent Backward-Facing Step Flows in Two-Dimensional Ducts and Channels," *Turbulent Shear Flows Conference 3*, Davis, CA, 1982.

[39]Eaton, J. K., and Johnston, J. P., "An Evaluation of Data for the Backward-Facing Step Flow," *1980/81 AFOSR-HTTM-Stanford Conference on Complex Turbulent Flows, 1980.*

[40]Arie, M., and Rouse, H., "Experiments on Two-Dimensional Flow over a Normal Wall," *Journal of Fluid Mechanics*, Vol. 1, 1956, pp. 129–141.

[41]Hussain, A. K. M. F., "Coherent Structures—Reality and Myth," *Physics of Fluids,* Vol. 26, 1983, pp. 2816–2850.